PHILOSOPHICAL TRANSACTIONS OF THE ROYAL SOCIETY B

rstb.royalsocietypublishing.org

Research

Cite this article: Khelfaoui M *et al*. 2014 Lack of the presynaptic RhoGAP protein oligophrenin1 leads to cognitive disabilities through dysregulation of the cAMP/PKA signalling pathway. *Phil. Trans. R. Soc. B* **369**: 20130160.
http://dx.doi.org/10.1098/rstb.2013.0160

One contribution of 35 to a Discussion Meeting Issue 'Synaptic plasticity in health and disease'.

Subject Areas:
behaviour, neuroscience, cellular biology, molecular biology

Keywords:
amygdala, presynaptic plasticity, adenylate cyclase, PKA, fasudil

Author for correspondence:
Yann Humeau
e-mail: yann.humeau@u-bordeaux2.fr

†Present address: Département des neurosciences fondamentales, CMU, Geneva, Switzerland.

Electronic supplementary material is available at http://dx.doi.org/10.1098/rstb.2013.0160 or via http://rstb.royalsocietypublishing.org.

Royal Society Publishing

Lack of the presynaptic RhoGAP protein oligophrenin1 leads to cognitive disabilities through dysregulation of the cAMP/PKA signalling pathway

Malik Khelfaoui[1,2,3,4], Frédéric Gambino[1,†], Xander Houbaert[5], Bruno Ragazzon[2,3], Christian Müller[4], Mario Carta[5], Frédéric Lanore[5], Bettadapura N. Srikumar[5], Philippe Gastrein[4], Marilyn Lepleux[5], Chun-Lei Zhang[5], Marie Kneib[1], Bernard Poulain[1], Sophie Reibel-Foisset[6], Nicolas Vitale[1], Jamel Chelly[2,3], Pierre Billuart[2,3], Andreas Lüthi[4] and Yann Humeau[1,5]

[1]Centre National de la Recherche Scientifique UPR3212, CNRS, Université de Strasbourg, Strasbourg 67084, France
[2]Institut Cochin, Université Paris Descartes, CNRS (UMR 8104), Paris 75014, France
[3]INSERM, U1016, Paris 75014, France
[4]Friedrich Miescher Institute for Biomedical Research, 4058 Basel, Switzerland
[5]Institut interdisciplinaire de neuroscience, CNRS UMR5297, University of Bordeaux, Bordeaux, France
[6]Plateforme d'hébergement et d'explorations fonctionnelles, IFR 37, Strasbourg 67084, France

Loss-of-function mutations in the gene encoding for the RhoGAP protein of oligophrenin-1 (OPHN1) lead to cognitive disabilities (CDs) in humans, yet the underlying mechanisms are not known. Here, we show that in mice constitutive lack of *Ophn1* is associated with dysregulation of the cyclic adenosine monophosphate/phosphate kinase A (cAMP/PKA) signalling pathway in a brain-area-specific manner. Consistent with a key role of cAMP/PKA signalling in regulating presynaptic function and plasticity, we found that PKA-dependent presynaptic plasticity was completely abolished in affected brain regions, including hippocampus and amygdala. At the behavioural level, lack of OPHN1 resulted in hippocampus- and amygdala-related learning disabilities which could be fully rescued by the ROCK/PKA kinase inhibitor fasudil. Together, our data identify OPHN1 as a key regulator of presynaptic function and suggest that, in addition to reported postsynaptic deficits, loss of presynaptic plasticity contributes to the pathophysiology of CDs.

1. Introduction

Mutations in more than 80 human X-linked genes have been implicated in cognitive disabilities (CDs), a condition estimated to affect 1–3% of the population [1–3]. Consistent with human genetics, most genetic mouse models of X-linked CD display learning and memory deficits [4,5]. Yet, it is still largely unclear how mutations in CD genes interfere with the function and plasticity of neuronal circuits.

Ophn1 mutations are causal for a syndromic form of CD, including cerebellum hypoplasia and an expansion of lateral ventricles [6–8]. Some of these phenotypes are reproduced in *Ophn1* mutant mice [9]. Importantly, both hyper- and hypo-expression of the oligophrenin1 (OPHN1) protein were found to be associated with CD [10], suggesting that Ophn1 dosage is important for controlling CD relevant signalling cascades. In rodents, *Ophn1* is expressed in the adult brain with higher expression levels in the hippocampus, cortex, amygdala, olfactory bulb and the cerebellum [9]. At the cellular level, *Ophn1* is expressed in both neurons and glial cells where it has been shown to interact with F-actin in cellular compartments concerned with active membrane movements such as growth cones,

filopodia and dendritic spines [9,11,12]. At synapses, OPHN1 is located in both pre- and postsynaptic compartments of excitatory and inhibitory synapses [9,13].

We recently discovered that the Rho GTPase-activating protein (RhoGAP) OPHN1 interacts with endophilin, amphyphisin and Cin85, thereby controlling clathrin-mediated endocytosis through the RhoA/Rho-associated protein kinase (ROCK) pathway [13]. Lack of OPHN1 was associated with a decrease in cellular endocytosis which was efficiently reversed by ROCK antagonist, suggesting that this cascade may participate in the pathophysiology of CD associated with *Ophn1* mutations. As expected from a general blockade of membrane trafficking, both membranous diffusion of postsynaptic [13–15] and presynaptic vesicular trafficking [13,16] were affected in neuronal cells in which acute or permanent deletions of *Ophn1* were introduced, suggesting important pre- and postsynaptic functions for OPHN1.

One of the major signalling pathways controlling different aspects of presynaptic function and plasticity is the cyclic adenosine monophosphate/phosphate kinase A (cAMP/PKA) pathway [17]. Some of cellular cAMP/PKA-dependent processes involve the regulation of Rho/RhoA signalling [18,19]. It is thus possible that the constitutive lack of OPHN1 could lead to a dysregulation of presynaptic PKA signalling with potentially widespread consequences on presynaptic function and plasticity.

We tested this hypothesis using *Ophn1*-deficient animals and found that constitutive lack of OPHN1 resulted in a profound dysregulation of the cAMP/PKA signalling pathway, and a complete abolishment of PKA-dependent presynaptic long-term plasticity in two brain areas important for different forms of learning and memory: the lateral amygdala (LA) and the hippocampus. At the behavioural level, both extinction- and context-dependent renewal of conditioned fear responses were severely impaired. Using fasudil, a clinically approved kinase inhibitor, we were able to rescue the behavioural deficits in Ophn1-deficient animals. These results thus suggest that, in parallel to alterations of postsynaptic function, presynaptic deficits induced by chronic dysregulation of PKA signalling may participate in the pathophysiology of Ophn1-related CDs.

2. Material and methods

(a) Animals

All experiments were performed using male *Ophn1*$^{-/y}$ and their control littermates *Ophn1*$^{+/y}$, housed in 12 L : 12 D with ad libitum feeding. Rim1$\alpha^{-/-}$ mice and wild-type littermates were kindly provided by Dr T.C. Südhof (Standford University, Palo Alto, CA, USA). Every effort was made to minimize the number of animals used and their suffering. The experimental design and all procedures were in accordance with the European guide for the care and use of laboratory animals and the animal care guidelines issued by the animal experimental committee of Paris, Strasbourg and Bordeaux Universities.

(b) Electrophysiology

(i) Amygdala slice preparation

Standard procedures were used to prepare 330 µm thick coronal slices from three- to four-week-old male wild-type or mutant mice (C57BL/6N background). Briefly, the brain was dissected in ice-cold artificial cerebrospinal fluid (ACSF), mounted on an agar block and sliced with a vibratome (Leica VT1200 s; Germany) at 4°C. Slices were maintained for 45 min at 35°C in an interface chamber containing ACSF equilibrated with 95% O_2/5% CO_2 and containing (in mM): 124 NaCl, 2.7 KCl, 2 $CaCl_2$, 1.3 $MgCl_2$, 26 $NaHCO_3$, 0.4 NaH_2PO_4, 18 glucose, 4 ascorbate and then for at least 45 min at room temperature before being transferred to a superfusing recording chamber.

(ii) Amygdala recordings

Whole-cell recordings from LA principal neurons were performed at 30–32°C in a superfusing chamber as previously described [20]. Neurons were visually identified with infrared video-microscopy using an upright microscope equipped with a 60× objective. Patch electrodes (3–5 MΩ) were pulled from borosilicate glass tubing and filled with a low-chloride solution containing (in mM): 140 Cs–methylsulfonate, 5 QX-314-Cl, 10 HEPES, 10 phosphocreatine, 4 Mg–ATP and 0.3 Na–GTP (pH adjusted to 7.25 with CsOH, 295 mOsm). For current-clamp experiments, Cs–methylsulfonate was replaced with equimolar K–gluconate. All experiments were performed in the presence of picrotoxin (100 µM). Monosynaptic excitatory postsynaptic currents (EPSCs) or excitatory postsynaptic potentials (EPSPs) exhibiting constant 10–90% rise times and latencies were elicited by stimulation of afferent fibres with a bipolar twisted platinum/10% iridium wire (25 µm diameter).

(iii) Data acquisition and analysis

Data were recorded with a Multiclamp 700B (Molecular Devices, USA), filtered at 2 kHz and digitized at 10 kHz. In all experiments, series resistance was monitored throughout the experiment, and if it changed by more than 15%, then the data were not included in the analysis. Data were acquired and analysed with pCLAMP10.2 (Molecular Devices). Changes were quantified by normalizing and averaging EPSC amplitude or EPSP slope during the last 5 min of the experiments relative to the 5 min of baseline prior to long-term potentiation (LTP) induction or drug application. All values are given as means ± standard error of the mean (s.e.m.). Statistical analysis was performed using R language and environment for statistical computing. Mean values were compared between genotypes using either unpaired Student's *t*-test or Mann–Whitney test as appropriate (SIGMAPLOT12, Systat Software).

(iv) Hippocampal slice preparation

Experiments were performed on parasagittal hippocampal slices (350 µM thick) from 19- to 24-day-old male *Ophn1*$^{-/y}$ mice and their *Ophn1*$^{+/y}$ littermates by using standard techniques [21]. Whole-cell voltage-clamp recordings (3.5–4.5 MΩ electrodes, −70 mV holding potential) were made at 30–32°C from hippocampal CA3 pyramidal cells visualized by infrared video-microscopy. Slices were perfused with an extracellular solution composed of (in mM): 125 NaCl, 2.5 KCl, 1.25 NaH_2PO_4, 26 $NaHCO_3$, 2.3 $CaCl_2$, 1.3 $MgCl_2$, 25 glucose, saturated with 95% O_2/5% CO_2. Bicuculline (10 µM) and D-AP5 (50 µM) were added to the bath to block, respectively, gamma aminobutyric acid A (GABAA) and *N*-methyl-D-aspartate (NMDA) receptors. The intracellular solution was composed of (in mM): 140 Ce–methanesulfonate, 2 $MgCl_2$, 4 NaCl, 5 phosphocreatine, 5 QX-314, 3 Na_2ATP, 0.2 EGTA, 10 HEPES, 0.33 GTP (pH 7.3). A glass microelectrode was placed in the dentate gyrus to stimulate mossy fibres. Stimulation intensity (200 µs pulse) was adjusted just above the sharp threshold for activation of a synaptic response. Mossy fibre (MF) synaptic currents were identified according to the following criteria: robust low-frequency facilitation, low release probability at 0.1 Hz, rapid single rise times (around 1 ms) and decays free of secondary peaks that may indicate the presence of polysynaptic contamination. At the end of each experiment, LCGG-1 (10 µM), a group II mGluR agonist, was used to verify the mossy fibre origin of the EPSCs. MF-LTP was induced using a high-frequency stimulation (HFS) protocol consisting of 100 stimulations at a frequency of 100 Hz,

repeated six times with a 10 s interval between trains in the presence of bicuculline (10 µM) and the NMDA receptor antagonist D-AP5 (50 µM). HFS was performed at baseline stimulation intensity, which consisted of a single pulse delivered every 10 s (0.01 Hz). Small, hyperpolarizing voltage steps were given before each afferent stimulus allowing online monitoring of input and series resistances.

(v) Data acquisition and analysis

Access resistance was less than 20 MΩ, and cells were discarded if it changed by more than 20%. Recordings were made using an EPC 9.0 or EPC 10 amplifier (HEKA Elektronik, Lambrecht/Pfalz, Germany) and were filtered at 0.5–1 kHz, digitized at 1–5 kHz and stored in a personal computer for additional analysis (Igor Pro 5.0; Wave Metrics, Lake Oswego, OR, USA). For statistical analysis values are presented as mean ± s.e.m. of n experiments. Either a paired or unpaired Student's t-test was used to define statistical differences between values, which were considered as significant at $p < 0.05$.

(c) PKA assay and cAMP measurements

PKA activity was measured using the PepTag non-radioactive cAMP-dependent protein kinase assay (V5340; Promega). Whole brain extracts or manually dissected cerebral structures were snap-frozen in liquid nitrogen. All samples were treated together, in duplicates, and corrected for protein concentration. The PepTag A1 peptide substrate was subjected to electrophoresis for 10–20 min in 1% (w/v) agarose gels, and the separated bands were photographed with a SynGene apparatus. The intensities of the bands were analysed with Gene Tool software. The basal PKA activity represents the difference between the ratios of phospho-/non-phospho forms with and without PKA inhibitor (PKI, 40 ng µl^{-1}, Promega). The same calculation in presence of 1 µM cAMP gave the total PKA activity. PKA activity in the presence of PKI was extremely low (less than 5%, figure 3*a*) confirming the high specificity of the assay. For cAMP levels analysis, frozen tissues were homogenized in a 0.1 M HCl solution and centrifuged at 900*g* at room temperature. cAMP content was determined with an enzyme immunometric assay kit (Assay Designs no. 900-066) following the manufacturer's instructions.

(d) Primary cell culture

Astroglial cells from *Ophn1* knockout (KO) animals and wild-type (WT) controls were prepared by standard procedures as previously described [9].

(e) Western blotting

An equal amount of protein (20 µg for neurons, 30–60 µg for whole brain) was separated on 10% acrylamide/bisacrylamide gels and transferred to nitrocellulose membranes. The blots were incubated over night at 4°C with the following primary antibodies: GluR1 phospho-Ser845 (Chemicon), GluR1 (Upstate), Tuj1 (Covance) and Ophn1 [11]. Antibody against synapsin phospho-site 1 (G257) was kindly provided by Prof. Fabio Benfenati. After incubation with the appropriate horseradish peroxidase-conjugated secondary antibodies (Dako, 1 : 10 000), immunoreactive bands were visualized by enhanced chemiluminescence detection (Thermo Scientific) and captured using an ImageQuant apparatus. The density of the signals was measured using ImageJ software. Phosphorylation rate was determined either as ratios between phosphorylated and total proteins or between phosphorylated proteins and the Tuj1 loading control.

(f) Protein kinase A subunit analysis

Whole-cell extracts were performed in radio-immunoprecipitation assay buffer completed with protease and phosphatase inhibitors (cOmplete and PhosSTOP; Roche Diagnostics). The concentration of proteins was determined by the Bradford method (Bio-Rad). Proteins were subjected to SDS–PAGE on 10% acrylamide gels and transferred onto nitrocellulose membranes (Amersham Pharmacia Biotech). Non-specific protein-binding sites were blocked by incubation for 1 h at room temperature in 50 mm Tris–HCl (pH 8), 150 mm NaCl and 0.1%, Tween 20 (TBS-T) containing 10% non-fat dry milk. Incubation with primary polyclonal antibodies (anti-R1α at 1 : 1000 (no. 610610, BD Biosciences), anti-Cα at 1 : 1000 (no. 610981, BD Biosciences) and anti-GAPDH at 1 : 1000 (sc-25778, Santa-Cruz)) was carried out in the same buffer overnight at 4°C. After washing in TBS-T, membranes were incubated for 1 h at room temperature with the peroxidase-conjugated anti-mouse IgG at 1 : 5000 (sc-2005, Santa-Cruz) or anti-rabbit IgG at 1 : 5000 (no. 7074S, Cell Signalling).

(g) Fear conditioning

Discriminative fear conditioning was performed on two- to three-month-old animals treated with the ROCK and PKA kinases inhibitor fasudil also known as HA1077 purchased from LC laboratories (Boston, MA, USA). Fasudil was dissolved in daily drinking water at 0.65 mg ml^{-1} and given orally three weeks before starting and during the fear tests.

Acquisition and retrieval of cued fear conditioning took place in two different contexts (context A and B) as previously described [22]. Briefly, on day 1, mice were submitted to a habituation session in context A, in which they received four representations of the CS^+ and the CS^- (CS^+: 30 s, consisting of 50 ms pips repeated at 0.9 Hz, 2 ms rise and fall, pip frequency 7.5 kHz; CS^-: same using either 3 kHz or white noise, 80 dB). Discriminative fear conditioning was performed the same day by pairing the conditioned stimulus (CS^+) with an unconditioned stimulus (US; 1 s foot-shock, 0.6 mA, 5 CS^+–US pairings; inter-trial interval: 20–180 s). The onset of the US coincided with the offset of the CS^+. The CS^- was presented after each CS^+/US association but was never reinforced (five CS^- presentations, inter-trial interval: 20–180 s). On day 2 and day 3, conditioned mice were submitted to an extinction test in context B during which they received four presentations of the CS^- and 12 presentations of the CS^+. A week later, mice were submitted to a fear retrieval test (context B, 4× CS^- and 4× CS^+) and finally to a fear renewal test (context A, 4× CS^- and 4× CS^+).

(h) Dendritic spine analysis

Neurons from standard coronal amygdala slices were filled intracellularly with 100 µM Alexa 594 with the patch pipette. Labelled neurons were imaged using an Olympus two-photon microscope and a 60× water-immersion objective. Eight-bit images were analysed using NeuronJ plugin from ImageJ software (http://rsbweb.nih.gov/ij/) with which length and density of spines were extracted.

(i) Reagents

Picrotoxin was from Sigma-Aldrich (Saint Quentin Fallavier, France), forskolin, cyclothiazide and H89 were from Tocris Bioscience (Bristol, UK), and QX-314 was from Alomone Labs Ltd. (Jerusalem, Israel). Tetrodotoxin was purchased from Latoxan and stock solution prepared in acetate buffer at pH 4.5. Nimodipine was from Ascent Scientific (Princeton, NJ, USA) and thapsigargin from Calbiochem (Merck KGaA, Darmstadt, Germany). HA-1077 was from purchase from LC laboratories (Woburn, MA, USA).

3. Results

(a) Brain-area-specific hyper-activation of protein kinase A signalling in *Ophn1*$^{-/y}$ mice

To measure PKA activity in brains of mutant mice, we first analysed whole-brain extracts using a PepTag assay (figure 1*a*,*b*).

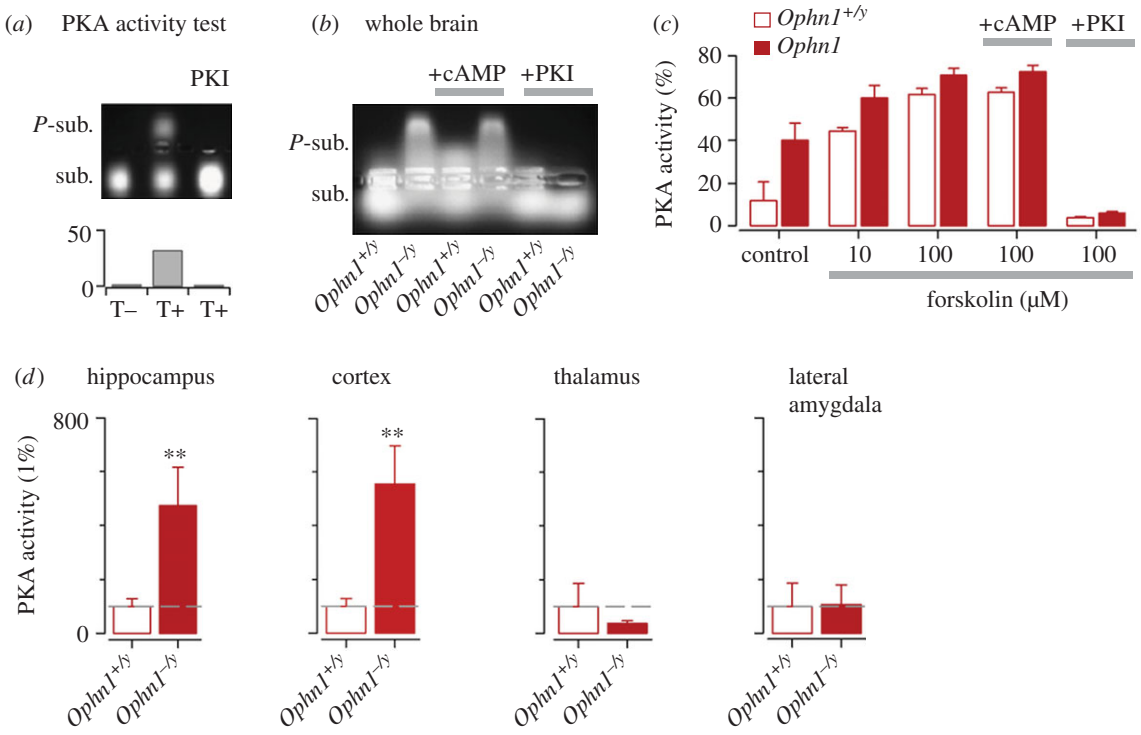

Figure 1. Brain-area-specific hyper-activation of PKA signalling in *Ophn1*$^{-/y}$ mice. (*a*) Characterization of the PepTag assay. (*b*) Basal PKA activity was determined in whole brain lysates from *Ophn1*$^{+/y}$ and *Ophn1*$^{-/y}$ mice using a PepTag assay. Activation of AC and inhibition of PKA was tested in presence of cAMP (1 µM) or PKI (40 ng µl^{-1}), respectively. (*c*) Summary graph illustrating the PKA activity levels under basal conditions and following AC activation by increasing concentrations of forskolin. Saturation of AC activation was controlled by addition of cAMP (1 µM) and test specificity by addition of PKI ($n = 6$). (*d*) PepTag assays were repeated on micro-dissected brain areas as indicated ($n = 3$ animals in each group). **$p < 0.01$.

Strikingly, basal PKA activity was increased approximately fourfold in brains from *Ophn1*$^{-/y}$ animals (PKA activity: *Ophn1*$^{+/y}$, 8 ± 3%; *Ophn1*$^{-/y}$, 33 ± 11%; $n = 4$, $p < 0.01$; figure 1*b*). Then, we tested for endogenous adenylate cyclase (AC) by forskolin (FSK) treatment in cultured KO and WT astroglial cells (figure 1*c*), and observed a strong increase in PKA activity in both genotypes. FSK-induced activation occluded any further increase by addition of cAMP (1 µM; figure 1*c*). All PKA activity was blocked by the PKA inhibitor PKI (1 µM) demonstrating the specificity of the assay (figure 1*c*).

Because PKA hyperactivity could reflect higher cAMP levels, we quantified cAMP concentrations in *Ophn1*$^{-/y}$ and *Ophn1*$^{+/y}$ brain extracts. cAMP concentrations were identical between genotypes ($p > 0.05$, $n = 3$ independent experiments; electronic supplementary material, figure S1*a*), suggesting that the higher PKA activity observed in mutant brains was not a consequence of upstream AC hyperactivity. In an attempt to further explore the origin of PKA overactivity, we tested the expression of ubiquitous PKA regulatory (R1α) and catalytic (Cα) PKA subunits [13], but did not observe any difference between KO and WT mice (see electronic supplementary material, figure S1*b*).

In order to obtain direct support for hyperactivity of synaptic PKA signalling, we analysed the phosphorylation levels of several key proteins in both pre- and postsynaptic compartments (see electronic supplementary material, figure S1*c*). First, based on previous reports demonstrating that mutations in the *Ophn1* gene were associated with alterations in α-amino-3-hydroxy-5-methyl-4-isoxazolepropionic acid-receptor (AMPAR) trafficking [13,14], a process which depends on AMPAR phosphorylation [23], we tested the phosphorylation state of AMPARs in *Ophn1*$^{+/y}$ and *Ophn1*$^{-/y}$ brain extracts using specific antibodies against phosphorylated forms of AMPARs [24] (see electronic supplementary material, figure S1*c*). We first observed that, even though the total amount of the AMPAR subunits GluA1 and GluA2 was similar in both genotypes (data not shown), PKA-mediated phosphorylation of AMPARs was higher in *Ophn1*$^{-/y}$ brains, when compared with WT animals. Using specific antibodies against phosphorylated forms of synapsins [25], we found that PKA activity was also increased in the presynaptic compartment (see electronic supplementary material, figure S1*c*).

Finally, using micro-dissected brain samples, we tested whether abnormal PKA activity was homogeneously present across *Ophn1*$^{-/y}$ brains or whether there were differences between brain areas. PKA activity was found to be higher in hippocampus (473 ± 142%, $p < 0.01$) and in cortex (555 ± 121%, $p < 0.01$; figure 1*d*), but not in lateral amygdala (LA), and in thalamus (figure 1*d*) or in cerebellum (data not shown), indicating that the constitutive lack of OPHN1 may specifically impact the function of different brain areas.

(b) Constitutive lack of OPHN1 abolishes PKA-dependent presynaptic long-term potentiation downstream of AC activation

In order to examine the physiological consequences of chronically elevated levels of PKA signalling, we first analysed synaptic function and plasticity in the lateral amygdala, a brain area receiving presynaptic inputs from brain areas with elevated (cortex) and normal (thalamus) PKA activity in *Ophn1* KO animals. Whole-cell current- and voltage-clamp recordings were obtained from LA principal neurons located in the dorsal subdivision of the LA [26–28]. Monosynaptic EPSCs or EPSPs at thalamo-LA and cortico-LA synapses were elicited by stimulating fibres from the internal capsule,

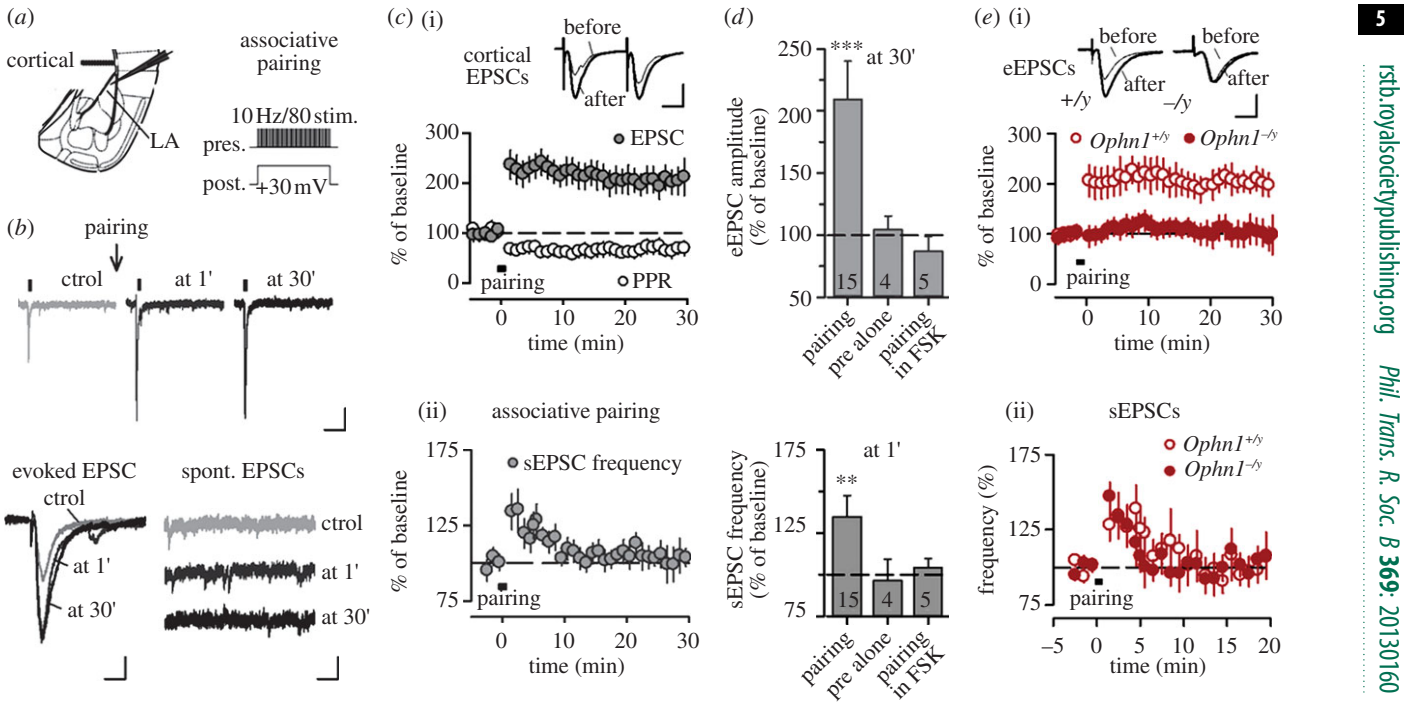

Figure 2. Constitutive lack of OPHN1 abolishes PKA-dependent presynaptic LTP downstream of AC activation. (*a*) Scheme of the experimental preparation and pairing protocol. Cortico-LA LTP was induced by pairing postsynaptic depolarization (8 s, +30 mV) with presynaptic stimulation (80 stimuli at 10 Hz). (*b*) Induction of presynaptic cortico-LA LTP leads to a persistent increase in EPSC amplitude and to a transient increase of sEPSC frequency. Scale bars, 50/50/25 pA and 300/5/25 ms (top/left/right panels). (*c*(i)) Presynaptic cortico-LA LTP is associated with a change in the PPR. Scale bars: 50 pA and 15 ms. (*c*(ii)) Associative pairing induces a transient increase of sEPSC frequency. (*d*) Characterization of pairing-induced cortico-LA LTP of the eEPSC (30 min time point) and the potentiation of sEPSC frequency (1 min time point). Both forms of plasticity are sensitive to pre-incubation with forskolin, and require coincident pre- and postsynaptic activity. See text for further details. Number of recorded cells is indicated. $^{**}p < 0.01$; $^{***}p < 0.001$. (*e*(i)) LTP induction in $Ophn1^{+/y}$ and $Ophn1^{-/y}$ animals. Scale bars, 50 pA and 5 ms. (*e*(ii)) LTP induction in both $Ophn1^{+/y}$ and $Ophn1^{-/y}$ animals leads to a transient increase in sEPSC frequency.

containing thalamic afferents or from the external capsule, containing cortical afferents (figure 2*a*) [29]. Interestingly, both inputs express LTP following cued fear conditioning [30,31].

Presynaptic PKA-dependent LTP can be induced in the cortico-LA pathway [32,33]. Presynaptic cortico-LA LTP can be induced by pairing stimulation of the cortico-LA pathway with concurrent stimulation of thalamic inputs [28] or with postsynaptic depolarization of LA principal neurons [34] (figure 2*a–c*). This form of LTP was associated with a change in the postsynaptic response to paired-pulse stimulation (paired-pulse ratio, PPR; figure 2*c*(i)) and was blocked by pre-incubation with FSK (figure 2*d*). Immediately after the pairing protocol, we also noted a transient increase in the frequency of spontaneous excitatory postsynaptic currents (sEPSCs) returning to baseline levels within 10–15 min (figure 2*b*,*c*(ii)). Similar to LTP of evoked EPSC amplitude, potentiation of sEPSC frequency did not occur in the absence of postsynaptic depolarization or in the presence of FSK (figure 2*d*).

Next, we examined LTP of evoked and spontaneous synaptic transmission at cortico-LA synapses in $Ophn1^{-/y}$ animals and wild-type littermates. Although LTP of evoked transmission was normal in $Ophn1^{+/y}$ controls ($198 \pm 17\%$, $n = 7$, $p < 0.05$; figure 2*e*), it was completely absent in $Ophn1^{-/y}$ mice ($107 \pm 8\%$, $n = 10$, $p < 0.05$; figure 2*e*). By contrast, and consistent with normal cAMP levels in $Ophn1^{-/y}$ mice, pairing-induced potentiation of sEPSC frequency were similar in $Ophn1^{+/y}$ and $Ophn1^{-/y}$ littermates (figure 2*e*(ii)). Together, these findings indicate that lack of OPHN1 results in a failure in PKA-mediated control of glutamate release downstream of AC activation.

(c) Selective loss of PKA-dependent presynaptic long-term plasticity in $Ophn1^{-/y}$ mice

The above findings show that at cortico-LA synapses, AC activity controls spontaneous and evoked glutamate release via two distinct mechanisms, only the latter being OPHN1-dependent. To further characterize these two cellular pathways, we analysed evoked and spontaneous glutamate release following pharmacological activation of AC by FSK (10 µM) while stimulating the external capsule (figure 3*a–g*). A brief application of FSK (10 min) led to a long-term increase in both evoked (EPSC amplitude) and spontaneous (EPSC frequency) glutamate release (figure 3*b*,*c*). However, when challenged by pharmacological and molecular manipulations previously reported to block the FSK effect on evoked release (e.g. manipulations of the PKA/Rim1α/L-type voltage-gated calcium channel pathway) [33,35], spontaneous release was still increased by FSK (figure 3*d–f*), and occluded by pre-incubation of slices with thapsigargin (5 µM), a blocker of Ca^{2+} stores (figure 3*f*). Importantly, the increase in sEPSC frequency was independent of PKA activity (figure 3*e*), suggesting that the two pathways diverge after AC activation.

Consistent with the pairing-induced increase in sEPSC frequency preserved in $Ophn1^{-/y}$ mice (figure 2*e*(ii)), sEPSC frequency was equally increased by brief application of FSK in both genotypes (figure 3*g*(i)). Next, in order to test if postsynaptic PKA activity participates in FSK-induced potentiation at cortico-LA synapses, we introduced the PKI peptide, an efficient PKA blocker (10 µM) through a patch pipette into the postsynaptic cell for at least 20 min. Under these conditions, normal FSK-induced potentiation of evoked transmission was

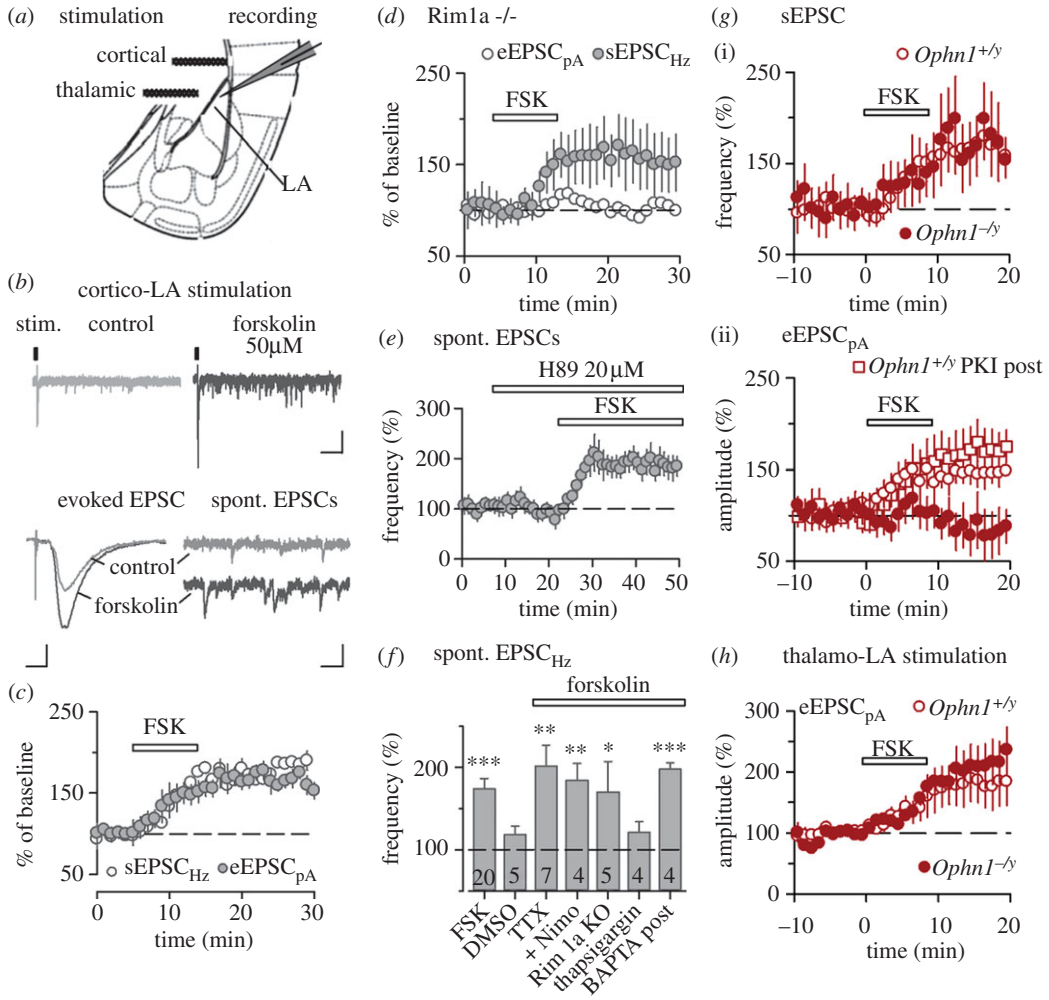

Figure 3. Selective loss of PKA-dependent presynaptic long-term plasticity in *Ophn1*$^{-/y}$ mice. (*a*) Scheme of the experimental preparation. (*b*) Typical recordings illustrating the effect of forskolin on evoked and spontaneous EPSCs. Scale bars, 50 pA and 300/5/25 ms (top/left/right panels). (*c*) Forskolin (FSK) enhances evoked synaptic transmission (eEPSC$_{pA}$) and spontaneous synaptic activity (sEPSC$_{Hz}$; $n = 13$). (*d*) Constitutive deletion of the presynaptic protein Rim1α does not block the FSK effect on evoked release ($n = 5$). (*e*) Pre-incubation with the PKA blocker H89 (20 µM) does not occlude the FSK-induced potentiation of sEPSC frequency ($n = 20$). (*f*) Pharmacological characterization of the FSK-induced potentiation of sEPSC frequency. Number of recorded cells is indicated. *$p < 0.05$; **$p < 0.01$; ***$p < 0.001$. (*g*(i)) Forskolin enhances sEPSC frequency in both *Ophn1*$^{+/y}$ (open circles) and *Ophn1*$^{-/y}$ (filled circles) animals ($n = 8$ and 8 cells). (*g*(ii)) Forskolin enhances evoked synaptic transmission in *Ophn1*$^{+/y}$ (open circles), but not in *Ophn1*$^{-/y}$ (filled circles) animals ($n = 5$ and 8 cells). Postsynaptic PKI infusion had no effect on the FSK-induced potentiation in *Ophn1*$^{+/y}$ animals (open squares; $n = 5$). (*h*) FSK-induced potentiation at thalamo-LA synapses was normal in *Ophn1*$^{-/y}$ animals ($n = 6$ and 5).

observed in *Ophn1*$^{+/y}$ mice (control: 147 ± 12%, $n = 6$, PKI: 165 ± 26%, $n = 5$, $p > 0.05$; figure 3*g*(ii)). Strikingly, however, when tested in *Ophn1*$^{-/y}$ mice, FSK-induced potentiation of evoked transmission was completely abolished (84 ± 25%, $n = 8$, $p > 0.05$; figure 3*g*(ii)).

Finally, to test whether loss of presynaptic regulation by PKA generalized to another converging excitatory synaptic input onto LA principal neurons, we examined the effect of FSK application on thalamo-LA synapses (figure 3*a*). In keeping with normal thalamic PKA activity in *Ophn1*$^{-/y}$ mice (figure 1*d*), FSK-induced LTP of evoked synaptic transmission was not impaired in *Ophn1*$^{-/y}$ mice (*Ophn1*$^{+/y}$: 182 ± 37%, *Ophn1*$^{-/y}$: 214 ± 35%, $n = 6$ and 5, $p > 0.05$; figure 3*h*), suggesting that at these thalamo-LA synapses AC/PKA-mediated control of neurotransmitter release was preserved.

(d) Lack of OPHN1 abolishes presynaptic long-term potentiation in hippocampus

Hippocampus is among the brain structures in which PKA activity was strongly increased in *Ophn1*$^{-/y}$ mice. PKA-dependent forms of presynaptic LTP exist at synaptic contacts between dentate gyrus granule cells and CA3 pyramidal neurons—the so-called mossy fibre terminals [36,37]. Presynaptic mossy fibre LTP requires Rim1α [38] and is regulated by presynaptic kainate receptors [39], thus strongly resembling presynaptic LTP at cortico-LA synapses [28,33]. We thus examined synaptic transmission and plasticity at hippocampal mossy fibre synapses (figure 4*a*). Using a minimal stimulation approach, we did not find any difference in basic synaptic properties between *Ophn1*$^{-/y}$ mice and littermate controls including both pre- and postsynaptic read-outs (electronic supplementary material, figure S2*a–c*). To examine mossy fibre LTP, we applied a tetanization protocol (100 Hz, 1 s, repeated six times with 10 s intervals), which induced short-term potentiation (STP) followed by LTP, two AC/PKA-dependent forms of plasticity in *Ophn1*$^{+/y}$ mice [40,41] (figure 4*b*). In stark contrast, both STP and LTP were largely absent in *Ophn1* mutant mice (at 1 min: *Ophn1*$^{+/y}$, 347 ± 91%; *Ophn1*$^{-/y}$, 173 ± 63%, $p < 0.05$; at 30 min: *Ophn1*$^{+/y}$, 160 ± 30%; *Ophn1*$^{-/y}$, 115 ± 35%, $p < 0.05$; figure 4*c*). Thus, consistent with the observed brain-area-specific hyperactivity of the PKA signalling pathway, lack of

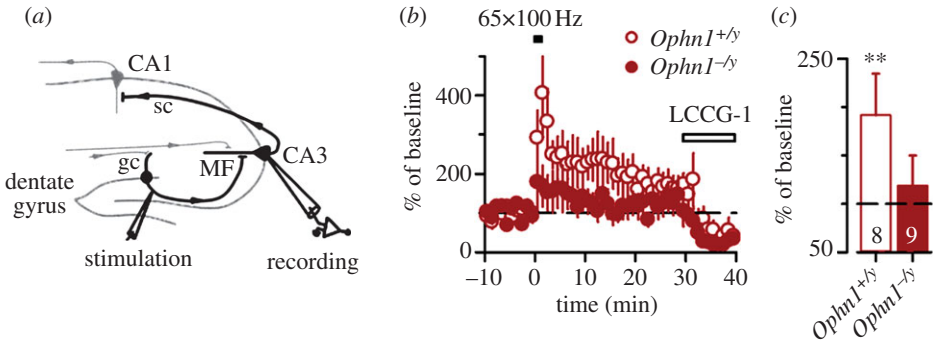

Figure 4. Lack of OPHN1 abolishes presynaptic LTP in hippocampus. (*a*) Scheme of the experimental preparation showing the placement of stimulating (gc) and recording electrodes (CA3). (*b*) Mossy fibre (MF)-LTP is absent in *Ophn1*$^{-/y}$ mice. (*c*) Summary bar graphs illustrate absence of LTP in *Ophn1*$^{-/y}$ animals. The number of recorded cells is indicated. $^{**}p < 0.01$.

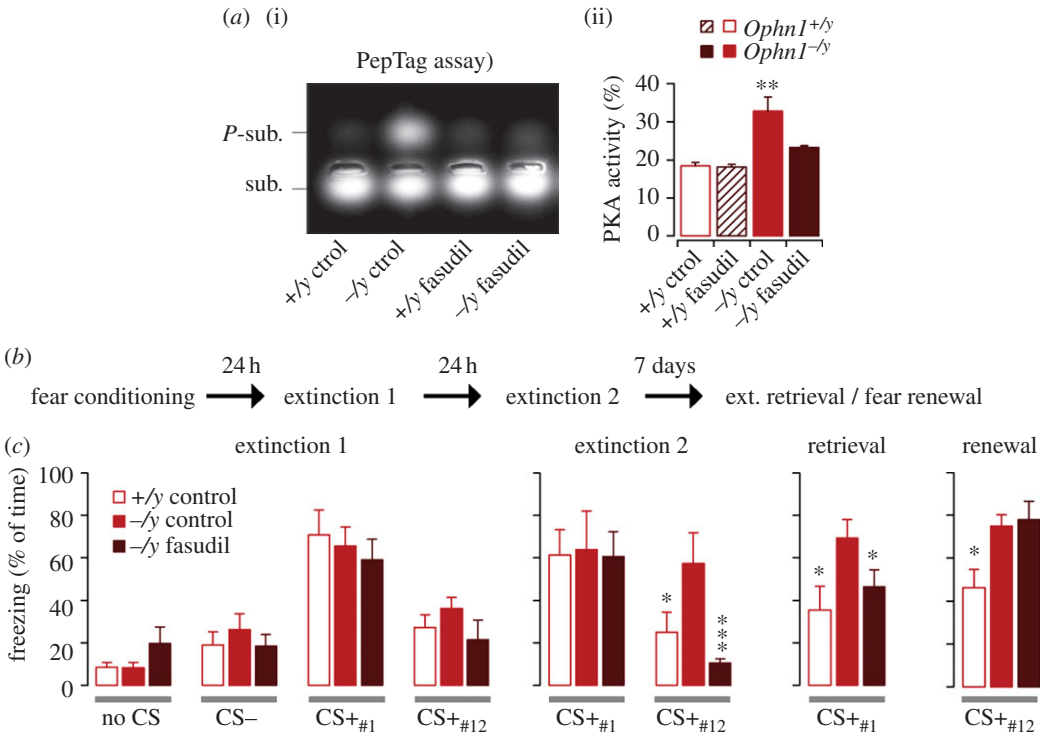

Figure 5. PKA inhibitor rescues impaired fear learning in *Ohpn1*$^{-/y}$ mice. (*a*(i)) PepTag assay was performed on brain extracts obtained from control and fasudil-treated animals. (*a*(ii)) Mean PKA activity values obtained in subgroups of *Ophn1*$^{+/y}$ ($n = 3$) and *Ophn1*$^{-/y}$ ($n = 3$) animals tested in figure 1*d*. Fasudil was applied as specified in the Material and methods section. (*b*) Time schedule of cued fear conditioning and extinction protocols. (*c*) Mean freezing levels observed in *Ophn1*$^{+/y}$ ($n = 5$), *Ophn1*$^{-/y}$ ($n = 5$) and fasudil-treated *Ophn1*$^{-/y}$ mice ($n = 8$). Fourty eight hours after cued fear conditioning, *Ophn1*$^{-/y}$ mice exhibit impaired within-session extinction ($CS^{+}_{\#12}$ in extinction 2), which was rescued by fasudil treatment. Similarly, impaired long-term extinction memory in *Ophn1*$^{-/y}$ mice was restored by fasudil treatment.

presynaptic PKA-dependent long-term plasticity generalizes across multiple brain areas in *Ophn1*$^{-/y}$ mice suggesting that impaired presynaptic plasticity might represent a hallmark of OPHN1-associated CDs.

(e) PKA inhibitor rescues impaired fear learning in *Ophn1*$^{-/y}$ mice

To examine the behavioural consequences of increased presynaptic PKA activity and lack of presynaptic long-term plasticity on amygdala- and hippocampus-dependent learning and memory, we analysed the acquisition, retrieval and extinction of classical fear conditioning in *Ophn1*$^{-/y}$ and *Ophn1*$^{+/y}$ animals (figure 5). Both *Ophn1*$^{+/y}$ and *Ophn1*$^{-/y}$ mice exhibited low freezing levels before conditioning (data not shown), and normal freezing levels when tested 24 h after pairing of the auditory conditioned stimulus with the US (mild foot-shock; extinction 1 in figure 5*b*,*c*). Thus, consistent with the proposed modulatory role for cortico-LA LTP in fear conditioning [20,22], lack of OPHN1 was not associated with a deficit in conditioned fear behaviour. However, although *Ophn1*$^{+/y}$ mice submitted to repeated non-reinforced CS presentations showed clear within-session fear extinction (extinction 2 in figure 5*b*,*c*), which resulted in the formation of a long-term extinction memory (extinction retrieval, figure 5*c*), *Ophn1*$^{-/y}$ mice exhibited significant less within- and across-session extinction suggesting a deficit in the acquisition and/or consolidation of extinction memories. Notably, when inducing fear renewal by placing the animals back into the conditioning context, *Ophn1*$^{-/y}$ mice showed markedly higher freezing levels in the presence of both the CS^{-} and the CS^{+} (CS^{-}: figure 5*c* and data not shown). This is consistent with the observed deficit in presynaptic hippocampal mossy fibre potentiation, because fear extinction and context-dependent

fear renewal not only require an intact amygdala but are also hippocampus-dependent [42].

To test whether overactivation of PKA signalling causally contributed to the impaired fear learning, we treated *Ophn1*$^{-/y}$ mice and control littermates with the clinically approved PKA inhibitor fasudil for three weeks. Indeed, fasudil treatment was able to reduce PKA activity in *Ophn1*$^{-/y}$ mice (figure 5*a*). Although fasudil did not affect acquisition, extinction and extinction retrieval in littermate controls (freezing levels in *Ophn1*$^{+/y}$: CS^{+}#1$_{ext1}$ ctrl: 71 $\pm$ 12%, fasudil: 51 $\pm$ 5%; CS^{+}#12$_{ext2}$ ctrl: 25 $\pm$ 15%, fasudil: 10 $\pm$ 3%; CS^{+}#1$_{retrieval}$ ctrl: 44 $\pm$ 14%, fasudil: 27 $\pm$ 12%, $n = 5$ and 7, $p = 0.114$, $p = 0.113$ and $p = 0.365$, respectively), it completely reversed the extinction memory deficit seen in *Ophn1*$^{-/y}$ mice (figure 5*c*). Fasudil treatment had no effect on fear renewal independent of the genotype (figure 5*c* and data not shown).

4. Discussion

Our study demonstrates that constitutive lack of OPHN1 leads to abnormally high levels of PKA activity and to the uncoupling of the cAMP/PKA signalling pathway from synaptic function and plasticity. In particular, presynaptic PKA-dependent long-term plasticity in both amygdala and hippocampus was severely compromised in the absence of OPHN1.

It is well established that cAMP signalling plays a central role in neuronal plasticity and learning [43,44]. This includes both acute effects mediated through activation of PKA and long-term changes involving transcriptional regulation [45]. Indeed, PKA activation leads to the phosphorylation and activation of the cAMP response element binding protein (CREB), which is required for activity-dependent gene transcription during the late phase of postsynaptic LTP and controls neuronal excitability (for a review, see [45]), two mechanisms which could also contribute to the behavioural deficits observed in *Ophn1*-deficient mice. In addition, PKA signalling is involved in hippocampal LTD [46,47]. However, because dihydroxyphenylglycine (DHPG)-induced LTD is normal in *Ophn1*$^{-/y}$ mice [9], it is unlikely that a deficit in hippocampal NMDAR-dependent LTD plays a major role in the impairment of contextual fear memory. Interestingly, normal learning and memory requires cAMP/PKA signalling to operate in an optimal range. Either too much activity or too little activity results in learning deficits, suggesting the existence of complex compensatory feedback mechanisms. Accordingly, modulators of cAMP phosphodiesterases (PDEs) have been successfully used to correct for memory deficits induced by up- or downregulations of PKA signalling [43,48]. Mice expressing a constitutively active form of Gαs in forebrain neurons exhibit lower brain cAMP levels because of an increase in PKA-dependent PDE activity [48]. Gαs overexpressing animals exhibited a deficit in one-trial fear learning which could be overcome by multiple learning trials and corrected by application of a PKA inhibitor [48]. In keeping, we found that *Ophn1*-deficient mice show normal fear learning in a multi-trial learning paradigm, but severely compromised extinction learning, another form of learning depending on cAMP/PKA signalling [49]. Interestingly, genetic inhibition of PKA in the forebrain was shown to facilitate learning of fear extinction in mice [49], with a pronounced effect within extinction sessions, suggesting a crucial role of PKA signalling in some fast CREB independent and behaviourally relevant plasticity processes such as the one reported here.

Because contextual fear conditioning partially depends on hippocampal structures [50], and is also affected by manipulations of PKA signalling [51], we propose that both amygdala- and hippocampus-related deficits contribute to the physiological and behavioural phenotype of *Ophn1*$^{-/y}$mice. We cannot exclude, however, that functional deficits in other brain areas, such as the medial prefrontal cortex [52,53], also contribute to the impaired formation of long-term extinction memories.

Our data also demonstrate that treatment with fasudil, a clinically approved inhibitor of the PKA and RhoA/ROCK pathways, can rescue, at least in part, the biochemical and behavioural phenotype caused by the constitutive lack of OPHN1. The behavioural rescue could be explained by an action of fasudil on PKA and/or ROCK. Indeed, we previously showed that in *Ophn1*$^{-/y}$ mice not only PKA but also ROCK activity is upregulated [13]. Thus, the behavioural deficits induced by constitutive absence of OPHN1 are not caused by irreversible developmental deficits, but most likely reflect compensatory changes in signalling pathways that can be reversed acutely by pharmacological interventions.

While previous work has mainly focused on the role of OPHN1 in postsynaptic plasticity mechanisms, our study reveals that lack of OPHN1 has deleterious consequences on presynaptic PKA-dependent LTP in both amygdala and hippocampus. Even though LA projection neurons in *Ophn1*$^{-/y}$ mice exhibited postsynaptic deficits (see below), we believe that the lack of presynaptic LTP cannot be accounted for by postsynaptic factors. Most importantly, we found that in wild-type mice pairing of pre- and postsynaptic activity resulted in the simultaneous induction of two forms of associative presynaptic plasticity: a cAMP- and PKA-dependent increase in evoked synaptic transmission and a cAMP dependent, but PKA-independent increase in spontaneous synaptic transmission. Lack of OPHN1 resulted in the selective ablation of PKA-dependent LTP of evoked transmission with no effect on plasticity of spontaneous transmission. Together, with the fact that postsynaptic NMDA responses were not reduced (electronic supplementary material, figure S3*d*,*e*), that postsynaptic LTP at thalamo-LA inputs and short-term synaptic plasticity during repetitive stimulation were normal (electronic supplementary material, figures S4 and S5), and that FSK-induced potentiation of evoked transmission was preserved in the presence of postsynaptic PKI, this strongly argues that lack of OPHN1 leads to a dysregulation of presynaptic PKA signalling.

In hippocampal slice preparations, acute downregulation of ophn1 expression using siRNA approaches leads to alterations in the density and morphology of postsynaptic spine density along with changes in AMPARs mobility and deficits in postsynaptic LTP [14]. Consistent with these results and with the fact that dendritic spine morphology is affected in several genetic mouse models for X-linked intellectual disabilities (ID), including *Il1rapl1* and *Ophn1* [9,54], this suggests an important role for deficits in postsynaptic function and plasticity in the pathophysiology of X-linked ID. Although LA projection neurons in *Ophn1*$^{-/y}$ mice also exhibited a significant decrease in spine density and an increase in spine length (electronic supplementary material, figure S3*a*,*b*), postsynaptic LTP at thalamo-LA inputs was normal, similar to previous findings at Schaffer collateral-CA1 synapses in the hippocampus of *Ophn1*$^{-/y}$ mice [9]. Together,

these data argue that in the constitutive mouse model, post-synaptic plasticity is preserved whereas presynaptic LTP is strongly compromised.

How could the constitutive absence of OPHN1 lead to pre synaptic dysfunction? In other cell types, activation of the Rho-GTPases Cdc42 and Rac depends on cAMP/PKA activity (for review see [55]). Thus, constitutive hyperactivity in this pathway might lead to adaptive changes eventually uncoupling Rho-GTPase signalling from its upstream control by PKA. Alternatively, because Rho-GTPases are important regulators of the synaptic actin cytoskeleton (for review see [56]), alterations in the presynaptic cytoskeleton may result in the mislocalization of various components of the cAMP/PKA pathway and its targets [55], thereby interfering with spatially compartmentalized signalling complexes.

Dysregulation of Rho-GTPase signalling is implicated in other forms of presynaptic plasticity. The Rho-GTPase Cdc42 has been identified as a crucial component of the signalling machinery underlying long-term homeostatic scaling of presynaptic release probability at the *Drosophila* neuromuscular junction [57]. Interestingly, both Cdc42-dependent homeostatic scaling and different forms of presynaptic LTP converge upon regulation of presynaptic voltage-dependent calcium channels [35,57,58]. This may suggest that lack of OPHN1 might result in a profound dysfunction of presynaptic regulatory signalling systems contributing to both long-term homeostatic and Hebbian forms of plasticity. Our findings indicate that deficits in presynaptic regulatory signalling pathways may be an important factor contributing to X-linked ID.

Acknowledgements. We acknowledge C. Herry and J. Courtin for their help in setting the behavioural test, and the Pole *in vivo* for its help in housekeeping the mouse lines.

Funding statement. This study was supported by grants from the Agence Nationale pour la Recherche (Y.H., J.C.), the European Neuroscience Institutes Network (Y.H.), the Novartis Research Foundation (A.L.), the National Center of Competences in Research 'SYNAPSY - The Synaptic Bases of Mental Diseases' supported by the Swiss National Science Foundation (A.L.), the European Union's Seventh Framework Programme no. 241995, project GENCODYS, and Sanofi Aventis.

References

1. Flint J. 1999 The genetic basis of cognition. *Brain* **122**, 2015–2032. (doi:10.1093/brain/122.11.2015)
2. Ropers HH, Hamel BC. 2005 X-linked mental retardation. *Nat. Rev. Genet.* **6**, 46–57. (doi:10.1038/nrg1501)
3. Chelly J, Khelfaoui M, Francis F, Chérif B, Bienvenu T. 2006 Genetics and pathophysiology of mental retardation. *Eur. J. Hum. Genet.* **14**, 701–713. (doi:10.1038/sj.ejhg.5201595)
4. Vaillend C, Poirier R, Laroche S. 2008 Genes, plasticity and mental retardation. *Behav. Brain Res.* **192**, 88–105. (doi:10.1016/j.bbr.2008.01.009)
5. Humeau Y, Gambino F, Chelly J, Vitale N. 2009 X-linked mental retardation: focus on synaptic function and plasticity. *J. Neurochem.* **109**, 1–14. (doi:10.1111/j.1471-4159.2009.05881.x)
6. Billuart P *et al*. 1998 Oligophrenin-1 encodes a rhoGAP protein involved in X-linked mental retardation. *Nature* **392**, 923–936. (doi:10.1038/31940)
7. Philip N, Chabrol B, Lossi AM, Cardoso C, Guerrini R, Dobyns WB, Raybaud C, Villard L. 2003 Mutations in the oligophrenin-1 gene (OPHN1) cause X linked congenital cerebellar hypoplasia. *J. Med. Genet.* **40**, 441–446. (doi:10.1136/jmg.40.6.441)
8. Zanni G *et al*. 2005 Oligophrenin 1 mutations frequently cause X-linked mental retardation with cerebellar hypoplasia. *Neurology* **65**, 1364–1369. (doi:10.1212/01.wnl.0000182813.94713.ee)
9. Khelfaoui M *et al*. 2007 Loss of X-linked mental retardation gene oligophrenin1 in mice impairs spatial memory and leads to ventricular enlargement and dendritic spine immaturity. *J. Neurosci.* **27**, 9439–9450. (doi:10.1523/JNEUROSCI.2029-07.2007)
10. Bedeschi MF *et al*. 2008 Association of syndromic mental retardation with an Xq12q13.1 duplication encompassing the oligophrenin 1 gene. *Am. J. Med. Genet. A* **146**, 1718–1724. (doi:10.1002/ajmg.a.32365)
11. Fauchereau F, Herbrand U, Chafey P, Eberth A, Koulakoff A, Vinet MC, Ahmadian MR, Chelly J, Billuart P. 2003 The RhoGAP activity of OPHN1, a new F-actin-binding protein, is negatively controlled by its amino-terminal domain. *Mol. Cell. Neurosci.* **23**, 574–586. (doi:10.1016/S1044-7431(03)00078-2)
12. Govek EE, Newey SE, Akerman CJ, Cross JR, Van der Veken L, Van Aelst L. 2004 The X-linked mental retardation protein oligophrenin-1 is required for dendritic spine morphogenesis. *Nat. Neurosci.* **7**, 364–372. (doi:10.1038/nn1210)
13. Khelfaoui M *et al*. 2009 Inhibition of RhoA pathway rescues the endocytosis defects in Oligophrenin1 mouse model of mental retardation. *Hum. Mol. Genet.* **18**, 2575–2583. (doi:10.1093/hmg/ddp189)
14. Nadif Kasri N, Nakano-Kobayashi A, Malinow R, Li B, Van Aelst L. 2009 The Rho-linked mental retardation protein oligophrenin-1 controls synapse maturation and plasticity by stabilizing AMPA receptors. *Genes Dev.* **23**, 1289–1302. (doi:10.1101/gad.1783809)
15. Nakano-Kobayashi A, Kasri NN, Newey SE, Van Aelst L. 2009 The Rho-linked mental retardation protein OPHN1 controls synaptic vesicle endocytosis via endophilin A1. *Curr. Biol.* **19**, 1133–1139. (doi:10.1016/j.cub.2009.05.022)
16. Powell AD, Gill KK, Saintot PP, Jiruska P, Chelly J, Billuart P, Jefferys JG. 2011 Rapid reversal of impaired inhibitory and excitatory transmission but not spine dysgenesis in a mouse model of mental retardation. *J. Physiol.* **590**, 763–767.
17. Seino S, Shibasaki T. 2005 PKA-dependent and PKA-independent pathways for cAMP-regulated exocytosis. *Physiol. Rev.* **85**, 1303–1342. (doi:10.1152/physrev.00001.2005)
18. Leemhuis J, Boutillier S, Schmidt G, Meyer DK. 2002 The protein kinase A inhibitor H89 acts on cell morphology by inhibiting Rho kinase. *J. Pharmacol. Exp. Ther.* **300**, 1000–1007. (doi:10.1124/jpet.300.3.1000)
19. Tkachenko E, Sabouri-Ghomi M, Pertz O, Kim C, Gutierrez E, Machacek M, Groisman A, Danuser G, Ginsberg MH. 2011 Protein kinase A governs a RhoA-RhoGDI protrusion-retraction pacemaker in migrating cells. *Nat. Cell Biol.* **13**, 660–667. (doi:10.1038/ncb2231)
20. Humeau Y *et al*. 2007 A pathway-specific function for different AMPA receptor subunits in amygdala long-term potentiation and fear conditioning. *J. Neurosci.* **27**, 10 947–10 956. (doi:10.1523/JNEUROSCI.2603-07.2007)
21. Rebola N, Carta M, Lanore F, Blanchet C, Mulle C. 2011 NMDA receptor-dependent metaplasticity at hippocampal mossy fiber synapses. *Nat. Neurosci.* **14**, 691–693. (doi:10.1038/nn.2809)
22. Shaban H *et al*. 2006 Generalization of amygdala LTP and conditioned fear in the absence of presynaptic inhibition. *Nat. Neurosci.* **9**, 1028–1035. (doi:10.1038/nn1732)
23. Shepherd JD, Huganir RL. 2007 The cell biology of synaptic plasticity: AMPA receptor trafficking. *Annu. Rev. Cell Dev. Biol.* **23**, 613–643. (doi:10.1146/annurev.cellbio.23.090506.123516)
24. Roche KW, O'Brien RJ, Mammen AL, Bernhardt J, Huganir RL. 1996 Characterization of multiple phosphorylation sites on the AMPA receptor GluR1 subunit. *Neuron* **16**, 1179–1188. (doi:10.1016/S0896-6273(00)80144-0)
25. Menegon A, Dunlap DD, Castano F, Benfenati F, Czernik AJ, Greengard P, Valtorta F. 2000 Use of phosphosynapsin I-specific antibodies for image analysis of signal transduction in single nerve terminals. *J. Cell Sci.* **113**, 3573–3582.

26. Bissière S, Humeau Y, Lüthi A. 2003 Dopamine gates LTP induction in lateral amygdala by suppressing feedforward inhibition. *Nat. Neurosci.* **6**, 587–592. (doi:10.1038/nn1058)
27. Sah P, Lopez De Armentia M. 2003 Excitatory synaptic transmission in the lateral and central amygdala. *Ann. N.Y. Acad. Sci.* **985**, 67–77. (doi:10.1111/j.1749-6632.2003.tb07072.x)
28. Humeau Y, Shaban H, Bissière S, Lüthi A. 2003 Presynaptic induction of heterosynaptic associative plasticity in the mammalian brain. *Nature* **423**, 841–845. (doi:10.1038/nature02194)
29. LeDoux JE. 2000 Emotion circuits in the brain. *Annu. Rev. Neurosci.* **23**, 155–184. (doi:10.1146/annurev.neuro.23.1.155)
30. Rumpel S, LeDoux J, Zador A, Malinow R. 2005 Postsynaptic receptor trafficking underlying a form of associative learning. *Science* **308**, 83–88. (doi:10.1126/science.1103944)
31. Tsvetkov E, Carlezon WA, Benes FM, Kandel ER, Bolshakov VY. 2002 Fear conditioning occludes LTP-induced presynaptic enhancement of synaptic transmission in the cortical pathway to the lateral amygdala. *Neuron* **34**, 289–300. (doi:10.1016/S0896-6273(02)00645-1)
32. Huang YY, Kandel ER. 1998 Postsynaptic induction and PKA-dependent expression of LTP in the lateral amygdala. *Neuron* **21**, 169–178. (doi:10.1016/S0896-6273(00)80524-3)
33. Fourcaudot E, Gambino F, Humeau Y, Casassus G, Shaban H, Poulain B, Luthi A. 2008 cAMP/PKA signaling and RIM1alpha mediate presynaptic LTP in the lateral amygdala. *Proc. Natl Acad. Sci. USA* **105**, 15 130–15 135. (doi:10.1073/pnas.0806938105)
34. Gambino F, Khelfaoui M, Poulain B, Bienvenu T, Chelly J, Humeau Y, Manzoni OJ. 2010 Synaptic maturation at cortical projections to the lateral amygdala in a mouse model of Rett syndrome. *PLoS ONE* **5**, e11399. (doi:10.1371/journal.pone.0011399)
35. Fourcaudot E, Gambino F, Casassus G, Poulain B, Humeau Y, Lüthi A. 2009 L-type voltage-dependent Ca^{2+} channels mediate expression of presynaptic LTP in amygdala. *Nat. Neurosci.* **12**, 1093–1095. (doi:10.1038/nn.2378)
36. Huang YY, Li XC, Kandel ER. 1994 cAMP contributes to mossy fiber LTP by initiating both a covalently mediated early phase and macromolecular synthesis-dependent late phase. *Cell* **79**, 69–79. (doi:10.1016/0092-8674(94)90401-4)
37. Weisskopf MG, Castillo PE, Zalutsky RA, Nicoll RA. 1994 Mediation of hippocampal mossy fiber long-term potentiation by cyclic AMP. *Science* **265**, 1878–1882. (doi:10.1126/science.7916482)
38. Castillo PE, Schoch S, Schmitz F, Südhof TC, Malenka RC. 2002 RIM1alpha is required for presynaptic long-term potentiation. *Nature* **415**, 327–330. (doi:10.1038/415327a)
39. Schmitz D, Mellor J, Breustedt J, Nicoll RA. 2003 Presynaptic kainate receptors impart an associative property to hippocampal mossy fiber long-term potentiation. *Nat. Neurosci.* **6**, 1058–1063. (doi:10.1038/nn1116)
40. Villacres EC, Wong ST, Chavkin C, Storm DR. 1998 Type I adenylyl cyclase mutant mice have impaired mossy fiber long-term potentiation. *J. Neurosci.* **18**, 3186–3194.
41. Huang YY, Kandel ER, Varshavsky L, Brandon EP, Qi M, Idzerda RL, Stanley McKnight G, Bourtchouladz R. 1995 A genetic test of the effects of mutations in PKA on mossy fiber LTP and its relation to spatial and contextual learning. *Cell* **83**, 1211–1222. (doi:10.1016/0092-8674(95) 90146-9)
42. Orsini CA, Kim JH, Knapska E, Maren S. 2011 Hippocampal and prefrontal projections to the basal amygdala mediate contextual regulation of fear after extinction. *J. Neurosci.* **31**, 17 269–17 277. (doi:10.1523/JNEUROSCI.4095-11.2011)
43. Li Y *et al*. 2009 Regulation of amygdalar PKA by beta-arrestin-2/phosphodiesterase-4 complex is critical for fear conditioning. *Proc. Natl Acad. Sci. USA* **106**, 21 918–21 923. (doi:10.1073/pnas.0906941106)
44. Selcher JC, Weeber EJ, Varga AW, Sweatt JD, Swank M. 2002 Protein kinase signal transduction cascades in mammalian associative conditioning. *Neuroscientist* **8**, 122–131. (doi:10.1177/1073858402080208)
45. Benito E, Barco A. 2010 CREB's control of intrinsic and synaptic plasticity: implications for CREB-dependent memory models. *Trends Neurosci.* **33**, 230–240. (doi:10.1016/j.tins.2010.02.001)
46. Brandon EP, Zhuo M, Huang YY, Qi M, Gerhold KA, Burton KA, Kandel ER, McKnight GS, Idzerda RL. 1995 Hippocampal long-term depression and depotentiation are defective in mice carrying a targeted disruption of the gene encoding the RI beta subunit of cAMP-dependent protein kinase. *Proc. Natl Acad. Sci. USA* **92**, 8851–8855. (doi:10.1073/pnas.92.19.8851)
47. Peineau S, Nicolas CS, Bortolotto ZA, Bhat RV, Ryves WJ, Harwood AJ, Dournaud P, Fitzjohn SM, Collingridge GL. 2009 A systematic investigation of the protein kinases involved in NMDA receptor-dependent LTD: evidence for a role of GSK-3 but not other serine/threonine kinases. *Mol. Brain* **2**, 22. (doi:10.1186/1756-6606-2-22)
48. Kelly MP, Cheung YF, Favilla C, Siegel SJ, Kanes SJ, Houslay MD, Abel T. 2008 Constitutive activation of the G-protein subunit Galphas within forebrain neurons causes PKA-dependent alterations in fear conditioning and cortical Arc mRNA expression. *Learn. Mem.* **15**, 75–83. (doi:10.1101/lm.723708)
49. Isiegas C, Park A, Kandel ER, Abel T, Lattal KM. 2006 Transgenic inhibition of neuronal protein kinase A activity facilitates fear extinction. *J. Neurosci.* **26**, 12 700–12 707. (doi:10.1523/JNEUROSCI.2743-06.2006)
50. Maren S. 2008 Pavlovian fear conditioning as a behavioral assay for hippocampus and amygdala function: cautions and caveats. *Eur. J. Neurosci.* **28**, 1661–1666. (doi:10.1111/j.1460-9568.2008.06485.x)
51. Schafe GE, Nadel NV, Sullivan GM, Harris A, LeDoux JE. 1999 Memory consolidation for contextual and auditory fear conditioning is dependent on protein synthesis, PKA, and MAP kinase. *Learn. Mem.* **6**, 97–110.
52. Quirk GJ, Mueller D. 2008 Neural mechanisms of extinction learning and retrieval. *Neuropsychopharmacology* **33**, 56–72. (doi:10.1038/sj.npp.1301555)
53. Herry C, Ferraguti F, Singewald N, Letzkus JJ, Ehrlich I, Lüthi A. 2010 Neuronal circuits of fear extinction. *Eur. J. Neurosci.* **31**, 599–612. (doi:10.1111/j.1460-9568.2010.07101.x)
54. Pavlowsky A *et al*. 2010 A postsynaptic signaling pathway that may account for the cognitive defect due to IL1RAPL1 mutation. *Curr. Biol.* **20**, 103–115. (doi:10.1016/j.cub.2009.12.030)
55. Howe AK. 2004 Regulation of actin-based cell migration by cAMP/PKA. *Biochim. Biophys. Acta* **1692**, 159–174. (doi:10.1016/j.bbamcr.2004.03.005)
56. Cingolani LA, Goda Y. 2008 Actin in action: the interplay between the actin cytoskeleton and synaptic efficacy. *Nat. Rev. Neurosci.* **9**, 344–356. (doi:10.1038/nrn2373)
57. Frank CA, Pielage J, Davis GW. 2009 A presynaptic homeostatic signaling system composed of the Eph receptor, ephexin, cdc42, and Cav2.1 calcium channels. *Neuron* **61**, 556–569. (doi:10.1016/j.neuron.2008.12.028)
58. Ahmed MS, Siegelbaum SA. 2009 Recruitment of N-type Ca^{2+} channels during LTP enhances low release efficacy of hippocampal CA1 perforant path synapses. *Neuron* **63**, 372–385. (doi:10.1016/j.neuron.2009.07.013)